Journal of Global Change Data & Discovery. 2023, 7(3): 242-251
www.geodoi.ac.cn

MODIS Global Leaf Area Index Product Reprocessing Dataset (2001–2021)

Liu, L.[1] Zhang, Y. H.[2*] Hu, Z. W.[2] Gao, X.[3] Wang, J. Z.[4] Wu, G. F.[2]

1. Guangdong Polytechnic of Industry & Commerce, Guangzhou 510510, China;
2. MNR Key Laboratory for Geo-Environmental Monitoring of Great Bay Area, Shenzhen University, Shenzhen 518060, China;
3. LREIS, Institute of Geographic Sciences and Natural Resources Research, Chinese Academy of Sciences, Beijing 100101, China
4. School of Artificial Intelligence, Shenzhen Polytechnic, Shenzhen 518055, China

Abstract: Global leaf area index (LAI) products provide important basic information for global climate change, carbon cycle, and sustainable development studies. In this study, based on MODIS LAI products, we designed a method to optimize current data. The results from the main algorithm with the maximum fraction of absorbed photosynthetically active radiation in a day were selected as high-quality results. A spatiotemporal filtering method that considers outliers and vegetation types was proposed to further modify the LAI data. Finally, a spatiotemporal continuous LAI dataset with high quality was produced. The data products revealed the distribution pattern of global LAI and elucidated its spatial and temporal variation characteristics under climate change from 2001 to 2021. Comparative analysis and validation of the results based on 280 validation points from the global LAI validation network showed that the reprocessed dataset had high product accuracy with a coefficient of determination (R^2) of 0.748, a bias of 0.12, and a root mean square error (RMSE) of 0.907. The dataset has a spatial resolution of 0.05° and a temporal resolution of 8 days and is archived in .tif format consisting of 1,239 files with a data size of 29.9 GB.

Keywords: MODIS; leaf area index; global change; spatial-temporal

DOI: https://doi.org/10.3974/geodp.2023.03.02

CSTR: https://cstr.escience.org.cn/CSTR:20146.14.2023.03.02

Dataset Availability Statement:

The dataset supporting this paper was published and is accessible through the *Digital Journal of Global Change Data Repository* at: https://doi.org/10.3974/geodb.2023.10.03.V1 or https://cstr.escience.org.cn/CSTR:20146.11.2023.10.03.V1.

Received: 08-03-2023; **Accepted:** 20-06-2023; **Published:** 25-09-2023

Foundations: National Natural Science Foundation of China (42201347); Shenzhen Science and Technology Program (JCYJ20220818101617037, 20220811173316001); Chinese Academy of Sciences (XDA23090503); China Postdoctoral Science Foundation (2022M712163); Guangdong Basic and Applied Basic Research Foundation (2021A1515110910, 2023A1515011273)

***Corresponding Author:** Zhang, Y. H. GYR-3820-2022, MNR Key Laboratory for Geo-Environmental Monitoring of Great Bay Area, Shenzhen University, zyhui@szu.edu.cn

Data Citation: [1] Liu, L., Zhang, Y. H., Hu, Z. W., *et al*. MODIS global leaf area index product reprocessing dataset (2001–2021) [J]. *Journal of Global Change Data & Discovery*, 2023, 7(3): 242–251. https://doi.org/10.3974/geodp.2023.03.02. https://cstr.escience.org.cn/CSTR:20146.14.2023.03.02.

[2] Liu, L., Zhang, Y. H., Hu, Z. W., *et al*. MODIS global leaf area index product reprocessing dataset (2001–2021) [J/DB/OL]. *Digital Journal of Global Change Data Repository*, 2023. https://doi.org/10.3974/geodb.2023.10.03.V1. https://cstr.escience.org.cn/CSTR:20146.11.2023.10.03.V1.

1 Introduction

The leaf area index (LAI) characterizes the sparseness of vegetation foliage and was first defined as the total surface area of one-sided foliage per unit surface area[1]. However, this definition is not applicable to vegetation with non-flat leaf surfaces such as coniferous vegetation. Chen and Black defined the LAI as the sum divided by two the surface area of green leaves per unit surface area[2]. In remote sensing, what is actually observed is half of the total surface area of the aboveground portion of green plants per unit area (plant area index, PAI), but it is still customarily referred to as the LAI[3]. It is a critical variable in processes such as photosynthesis, respiration, and precipitation interception[2, 3]. As a fundamental attribute of global vegetation, LAI has been listed as an essential climate variable by the global climate change research community[4].

Several global LAI products have been produced using satellite remote sensing data, including GLASS[5], GEOV2[6], and MODIS LAI[7]. Based on LAI products, spatiotemporal changes in global vegetation have been revealed[8], and global terrestrial ecosystem productivity products have been produced to support global carbon cycle studies and SDG assessments[9]. MODIS LAI products, as benchmark products, are the most widely used in global change studies. However, ground validation has shown that MODIS LAI products have larger uncertainties with significant anomalous fluctuations[10, 11]. The optimization of MODIS LAI products has been a concern for the scientific community. Yuan[12] and Wang *et al.*[13] proposed algorithms for optimizing MODIS LAI products. However, current algorithms rely on a priori filtering methods, and a priori knowledge is often influenced by the region and vegetation type, leading to over-optimization or under-fitting, causing incorrect vegetation changes, and impacting phenology extraction. The fraction of absorbed photosynthetically active radiation (FAPAR) is a companion variable for the MODIS LAI products[14]. Studies have shown that the inversion results of the LAI corresponding to the maximum FAPAR have high accuracy[15], providing quality criteria for further optimization of the MODIS LAI. Therefore, based on the two LAI/FAPAR results in one day, using the maximum FAPAR synthesis method and further conducting spatiotemporal filtering considering the vegetation types is an effective method for improving the data quality of MODIS LAI products. Finally this dataset utilizes two sets of MODIS LAI products, adopts the maximum FAPAR synthesis method for product fusion, considers the vegetation type to realize spatiotemporal filtering, and finally obtains the global LAI product with a spatial resolution of 0.05° and a temporal resolution of 8-day from 2001 to 2021.

2 Metadata of the Dataset

The metadata of the MODIS global lai product reprocessing dataset (2001–2021)[16] are summarized in Table 1. This includes details such as the full name, short name, authors, year of the dataset, temporal resolution, spatial resolution, data format, data size, data files, data publisher, and data-sharing policy, etc.

3 Methods

3.1 Data Sources

The production of these data relied on two MODIS LAI datasets, MOD15A2H and MYD15A2H, along with a land-cover product (MCD12Q1). The MODIS LAI products have a spatial resolution of 500 m and temporal resolution of 8 days. The inversion algorithm consists of a main and backup algorithm. The main algorithm utilized a lookup table

Table 1 Metadata summary of the MODIS global leaf area index product reprocessing dataset (2001–2021)

Items	Description
Dataset full name	MODIS global leaf area index product reprocessing dataset (2001–2021)
Dataset short name	SZU_ LAI
Authors	Liu, L. IVV-8131-2023, Guangdong Polytechnic of Industry & Commerce, llrain_li@126.com Zhang, Y. H. GYR-3820-2022, MNR Key Laboratory for Geo-Environmental Monitoring of Great Bay Area, Shenzhen University, zyhui@szu.edu.cn Hu, Z. W. AAX-7567-2021, MNR Key Laboratory for Geo-Environmental Monitoring of Great Bay Area, Shenzhen University, zwhoo@szu.edu.cn Gao, X. CPW-9851-2022, LREIS, Institute of Geographic Sciences and Natural Resources Research, Chinese Academy of Sciences, gxing@igsnrr.ac.cn Wang, J. Z. Q-4555-2019, School of Artificial Intelligence, Shenzhen Polytechnic, jzwang@szpt.edu.cn Wu, G. F. B-8735-2018, MNR Key Laboratory for Geo-Environmental Monitoring of Great Bay Area, Shenzhen University, guofeng.wu@szu.edu.cn
Geographical region	Global
Year	2001–2021
Temporal resolution	8-day, month, year
Spatial resolution	0.05°
Data format	.tif
Data size	29.9 GB
Data files	Leaf Area Index (LAI) dataset file, containing 8-day resolution data, monthly average and annual average data. MODIS_YYYYDOY_LAI.tif is the 8-day resolution leaf area index data, YYYY represents the year, DOY represents the Julian day, e.g., MODIS_2003009_LAI.tif is the leaf area index data of the 9th day of 2003; MODIS_YYYYMM_LAI.tif is the monthly average leaf area index data, YYYY represents the year, MM represents the month, e.g., MODIS_200301_LAI.tif is the average leaf area index data of January 2003 of January 2003; MODIS_YYYYY_LAI.tif is the annual average leaf area index data, YYYY represents the year, e.g., MODIS_2003_LAI.tif is the average leaf area index data of 2003
Foundations	National Natural Science Foundation of China (42201347); China Postdoctoral Science Foundation (2022M712163); Guangdong Province (2021A1515110910, 2023A1515011273); Chinese Academy of Sciences (XDA23090503); Shenzhen (JCYJ20220818101617037, 20220811173316001)
Data publisher	Global Change Research Data Publishing & Repository, http://www.geodoi.ac.cn
Address	No. 11A, Datun Road, Chaoyang District, Beijing 100101, China
Data sharing policy	(1) ***Data*** are openly available and can be free downloaded via the Internet; (2) End users are encouraged to use ***Data*** subject to citation; (3) Users, who are by definition also value-added service providers, are welcome to redistribute ***Data*** subject to written permission from the GCdataPR Editorial Office and the issuance of a ***Data*** redistribution license; and (4) If ***Data*** are used to compile new datasets, the 'ten per cent principal' should be followed such that ***Data*** records utilized should not surpass 10% of the new dataset contents, while sources should be clearly noted in suitable places in the new dataset[17]
Communication and searchable system	DOI, CSTR, Crossref, DCI, CSCD, CNKI, SciEngine, WDS/ISC, GEOSS

constructed from a three-dimensional (3D) radiative transfer model to invert the LAI. It uses atmospherically corrected MODIS reflectance and vegetation type data as inputs. The vegetation type data served as prior information to constrain the structural parameters of the vegetation, enabling the construction of different look-up tables. The valid land-cover types were as follows: (1) grass/cereal crops, (2) shrubs, (3) broadleaf crops, (4) savanna, (5) evergreen broadleaf forest, (6) deciduous broadleaf forest, (7) evergreen coniferous forest, and (8) deciduous coniferous forest. If the main algorithm failed, a backup algorithm was employed. The backup algorithm utilized the empirical relationship between the LAI and normalized difference vegetation index (NDVI) of a specific vegetation type to invert the LAI.

The MODIS LAI product provides quality control information (QC) that indicates the

quality of the LAI inversion. It includes information regarding the algorithm used for LAI inversion and whether it is affected by cloud or snow contamination. Images marked as clouds, snow, shadows, and cirrus were considered invalid and excluded from the dataset.

3.2 Algorithm

(1) Screening for high-quality LAI

1) Filtering the main algorithm inversion results: MODIS provides two sets of products: MOD15A2H and MYD15A2H. The quality layer of the products identifies the main algorithm inversion results, main algorithm inversion saturation results, use of alternate algorithms owing to the observation geometry, and other factors that lead to alternate algorithms. The main algorithm inversion results are thought to be of higher quality, and those of the two sets of products are first selected as candidate high-quality inversion values.

2) Filtering LAI value based on maximum FAPAR: When the LAI was retrieved, the FAPAR was output simultaneously, and the maximum FAPAR value was selected as the value in the 8-day synthesis process. The FAPAR and LAI synthesis analyses showed that lower FAPAR inversion values corresponded to lower inversion quality. In summary, we chose the LAI corresponding to the maximum FAPAR as the optimal inversion result for the main algorithm.

(2) Improvement in LAI temporal continuity

Temporal continuity processing was applied to address anomalous fluctuations in MODIS data. This study employed a 5-phase time period: LAI_{t-2}, LAI_{t-1}, LAI_t, LAI_{t+1}, and LAI_{t+2}. The following steps outline the specific process (Equation 1):

1) If LAI_t is an invalid value and the number of valid values in LAI_{t-2}, …, LAI_{t+2} is less than three, LAI_t remains as the invalid value.

2) If LAI_t is an invalid value and the number of valid values in LAI_{t-2}, LAI_{t+2} is three or four, then LAI_t is replaced by the average of the valid values.

3) If LAI_t is a valid value and the number of valid values within LAI_{t-2}, …, LAI_{t+2} is three and four, then an abnormally high or low value is determined as follows.

(a) If the LAI_t is greater than 1.5 times the average of the valid values, it is considered an abnormally high value and replaced with the average of the valid values.

(b) If LAI_t is less than 0.75 times the average of the valid values, it is considered an abnormally low value and replaced with the average of the valid values.

(c) In all other cases, the original value is retained.

4) If LAI_t is a valid value and the number of valid values within LAI_{t-2}, …, LAI_{t+2} is less than three, the original value is retained.

$$LAI_t^p = \begin{cases} Nan & N < 3 \quad LAI_t \text{ is } Nan \\ LAImean & N \geqslant 3 \\ LAI_t & N < 3 \\ LAImean \quad LAI_t > LAImean \times 1.5 & \\ LAImean \quad LAI_t < LAImean \times 0.75 & N \geqslant 3 \quad LAI_t \text{ is not } Nan \\ LAI_t \quad else & \end{cases} \tag{1}$$

(3) Downscaling methods

To accommodate global-scale studies, the dataset was downscaled to obtain data at a resolution of 0.05°. Existing downscaling methods often use statistical methods, such as nearest neighbor interpolation, and ignore the effects of non-vegetated pixels, such as water bodies, bare ground, and built-up areas. In this study, we proposed a downscaling method that considers the land cover type. We counted the number of vegetation cover pixels (Nv) in 12×12 pixels under the 0.05° grid and calculated the vegetation LAI (LAIv) of the total

vegetation pixels; then, the LAI under the 0.05° grid was calculated (Equation 2):

$$LAI_{0.05} = \frac{LAI_v}{144} \tag{2}$$

(4) Gap filling

We calculated a multi-year average of downscaled products from 2001 to 2021 to obtain the annual 8-day baseline LAI (LAI_b) data. Invalid pixels were filled considering the variable vegetation phenology in different years, assuming that the invalid pixels P and the corresponding baseline LAI pixel is P_b,

1) If the number of valid pixels around P is greater than four, the average valid values of 3×3 pixels around P are calculated as LAI_{tm} and the average valid values of 3×3 pixels around P_b are calculated as LAI_{bm}. The invalid values of the P pixels are then filled in, as (Equation 3):

$$LAI_t = LAI_b + LAI_{tm} - LAI_{bm} \tag{3}$$

2) Otherwise, the inverse value obtained by the MODIS backup algorithm is filled in.

3.3 Data Collection and Processing

The reprocessed LAI products from 2001 to 2021 were generated using two MODIS LAI datasets: MOD15A2H and MYD15A2H (Figure 1). The QA layer and maximum FAPAR synthesis method were employed to select high-quality results from both sets of products. Furthermore, using the five periods as sliding windows, the temporal consistency processing algorithm (Equation 1) was used to solve the abnormal fluctuations of the temporal sequence, which are common in products, and to improve the quality of LAI products. Considering the land-cover types, the high-quality vegetation LAI value averaging method (Equation 2) was used to produce data with a 0.05° spatial resolution, which is applicable to global change and earth system science research. Owing to data gaps caused by clouds, many nan values still exist. Based on the baseline leaf area data and considering the climatic changes, the nan values were further interpolated (Equation 3) to improve the spatial continuity of the product. Finally, a global spatiotemporal continuous LAI product with a temporal resolution of 8 d and a spatial resolution of 0.05° was generated for the period 2002–2022. Monthly and annual average products were also synthesized.

3.4 Validation

Ground-truth data were used to validate the dataset. Data validation requires high-quality ground references to validate the products[18]. The Committee on Earth Observation Satellites (CEOS) initiated the formation of Land Product Validation to construct the DIRECT V2.1 database[19]. This database aggregates global LAI measurements with high-precision measurements conducted according to the CEOS WGCV LPV LAI recommended method and upscaled to the 3 km×3 km range using high spatial resolution images to reduce the effect of spatial heterogeneity. The DIRECT V2.1 database, with 176 stations worldwide (seven vegetation types) and 280 LAI values covering the period 2000 to 2021, has become the primary database for satellite LAI product validation (Figure 2).

To verify the accuracy of the reprocessed dataset, this study utilized correlation and error analyses. To check the correlation between the ground truth data and product values, the coefficient of determination (R^2) was calculated.

$$R^2 = \frac{\sum_i^n \left(\hat{y}_i - y_i\right)^2}{\sum_i^n \left(y_i - \overline{y}_i\right)^2} \tag{4}$$

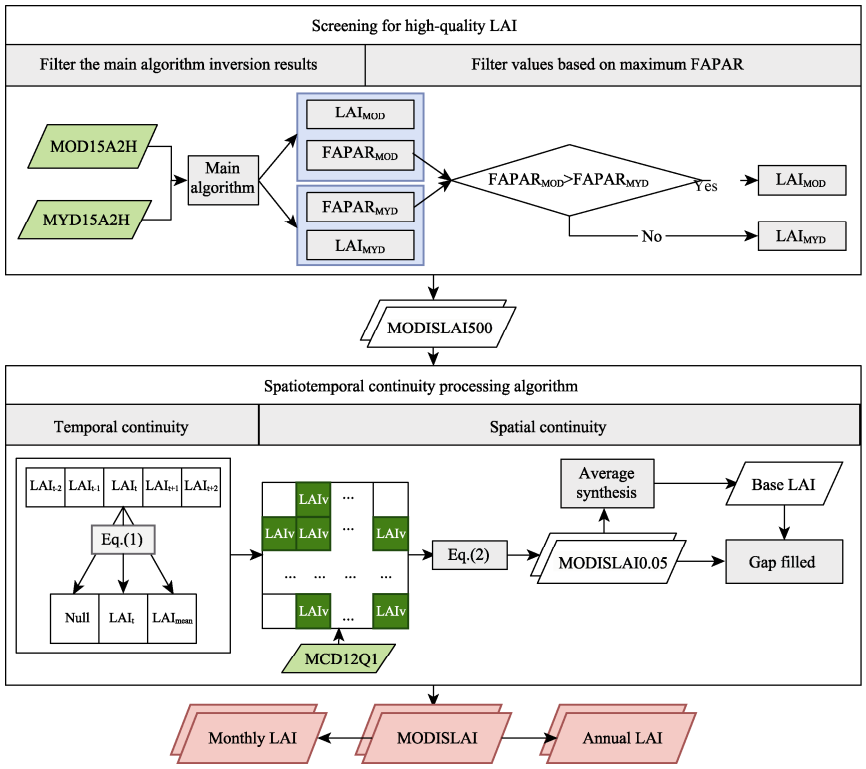

Figure 1 Flowchart of the dataset development

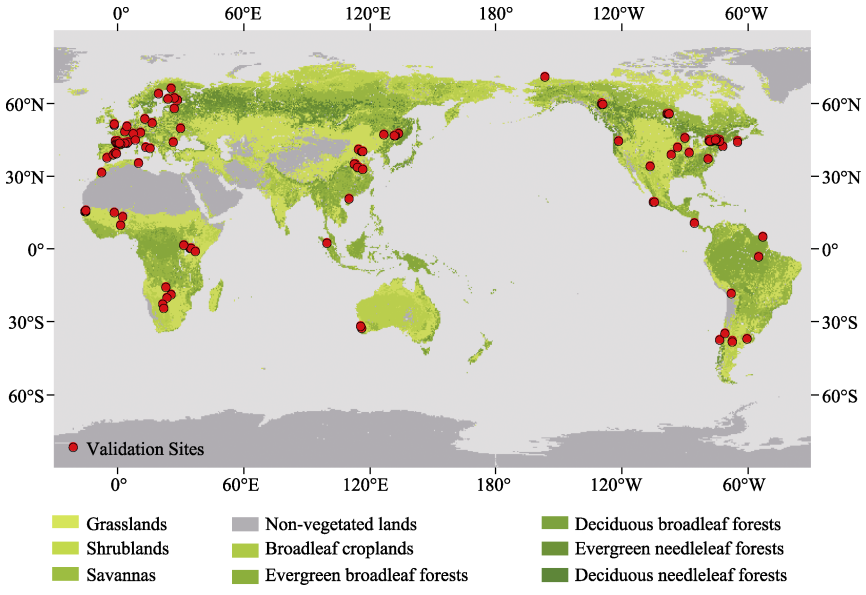

Figure 2 Map of the distribution of validation sites

where, y_i represents the ith sample value, the numerator represents the residuals predicted using the predicted value ($\hat{y}_i$), and the denominator represents the residuals obtained by predicting all data using the sample mean ($\overline{y}_i$). A larger R^2 value indicates that the residuals

of the model prediction results are smaller and the prediction is more effective.

The root mean square error (RMSE) and bias (bias) are calculated for the dataset result error. The RMSE can be used as an important indicator of the error between the true and predicted values, that is the smaller the RMSE value and the smaller the absolute value of the bias value, the better the validation result.

$$RMSE = \sqrt{\frac{1}{n}\sum_{i=1}^{n}\left(y_i - x_i\right)^2} \tag{5}$$

$$bias = \frac{1}{n}\sum_{i=1}^{n}\left(y_i - x_i\right) \tag{6}$$

where n represents the number of validation sample points, y represents the value to be validated, and x represents the true value.

4 Data Results and Validation

4.1 Data Composition

The global long-time series MODIS LAI reprocessing dataset consists of 8-day, monthly, and annual LAI datasets from 2001 to 2021. The dataset was saved in .tif format with a scale factor of 0.1.

Table 2 Dataset information

Folder name	File names	Data description	Data format	Number of data	Data size
8-Day LAI	MODIS_YYYYDOY_LAI	LAI data file for day DOY of year YYYY. The scale factor is 0.1 and the LAI value is the like element value × 0.1	.tif	966	23.3 GB
Month	MODIS_YYYYMM_LAI	Mean LAI data for month MM of year YYYY	.tif	256	6.08 GB
Year	MODIS_YYYY_LAI	Annual mean LAI data of year YYYY	.tif	21	519 MB

4.2 Data Analysis

(1) Spatial pattern

Figure 3 shows the global distribution of the average LAI for January, April, July, and October from 2001 to 2021. In January, a significant number of vacant values were observed owing to ice coverage in the Arctic region. Throughout the year, the Saharan Desert region in eastern Africa is devoid of LAI data. Conversely, regions near the equator, such as the Amazon rainforest, Central Africa, and Southeast Asia, exhibited consistently high LAI values close to seven in all four months. In July, the Northern Hemisphere, specifically eastern North America, central Eurasia, East Asia, and India, exhibited elevated LAI values.

(2) Temporal variation

The global LAI has exhibited an increasing trend from 2001 to 2021. Figure 4 illustrates this upward trajectory, with the average global and Northern Hemisphere LAI consistently increasing over time. Conversely, the LAI in the Southern Hemisphere remained stable after 2004 but experienced significant fluctuations from 2016 to 2019.

Figure 5 shows the temporal variation of the mean LAI in the global, Northern, and Southern Hemispheres. The Southern Hemisphere consistently exhibits higher LAI values throughout the year, ranging from 1.4 to 2.2, which are significantly greater than the global average (0.6 to 1.7) and that of the Northern Hemisphere (0.4 to 1.7). In the Southern Hemisphere,

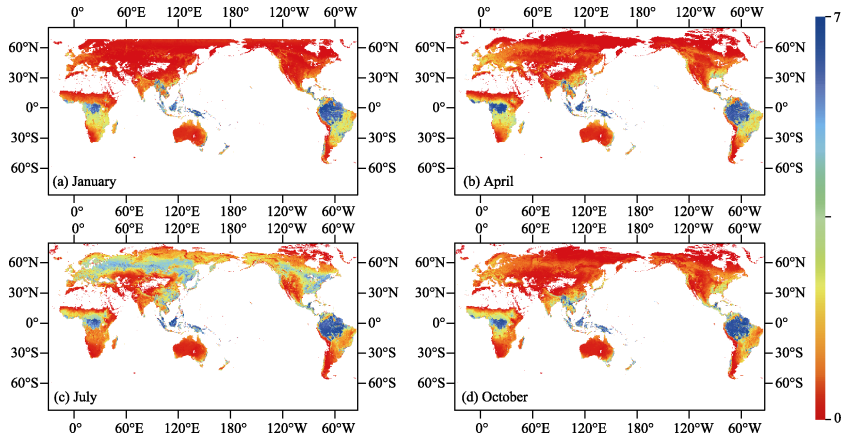

Figure 3 Global mean LAI maps derived from MODIS (0.05°) in January (a), April (b), July (c) and October (d), respectively (2001–2021)

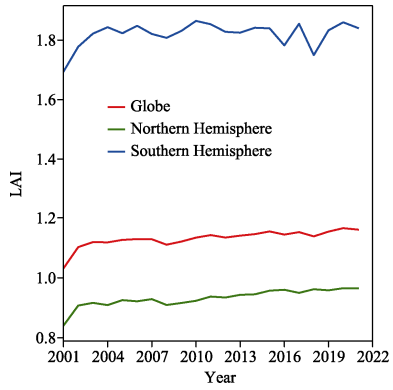

Figure 4 Temporal variation of global annually mean LAI (2001– 2021)

the LAI initially decreased and then increased over the course of the year, with the highest value of 2.2 occurring in January, and the lowest value of 1.4 occurring in July. Conversely, the Northern Hemisphere followed an opposite seasonal pattern, with the lowest LAI value (0.4) in January and the highest LAI value (1.7) in July. Both the global mean LAI and that of the Northern Hemisphere displayed similar seasonal variations and reached their maximum LAI values at similar times. However, the minimum global mean LAI value (0.6) was higher than the minimum LAI value observed for the Northern Hemisphere.

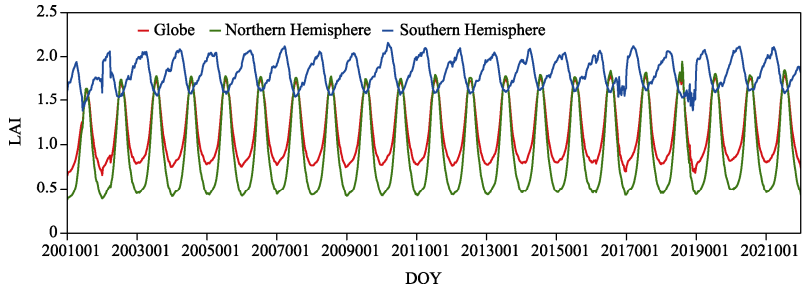

Figure 5 Temporal variation of global, Northern and Southern Hemisphere mean LAI (2001–2021)

An analysis was conducted to further investigate the spatial changes in the global LAI; the findings are presented in Figure 6. The areas exhibiting an increase in LAI were primarily concentrated in China, India, and Europe, with the maximum rate of increase recorded at 0.15 per year. Conversely, a decrease in LAI was observed near the Great Lakes in North America.

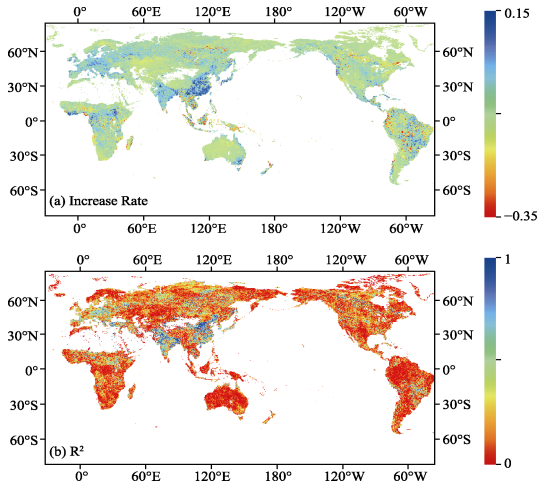

Figure 6 Map of long-term trend of the global LAI from 2001 to 2021

4.3 Data Validation

The product was validated using global LAI validation data; a scatter plot is shown in Figure 7. The product and ground-truth LAI showed good agreement; the linear fitting results were close to the 1:1 line, and the R^2 was 0.748, with a bias of 0.12 and RMSE of 0.907, which was better than the existing product accuracy[3] (R^2 = 0.615, bias = 0.13, RMSE = 1.16). The LAI was underestimated in broad-leaved evergreen forests because of the saturation effect that exists in remote sensing observations.

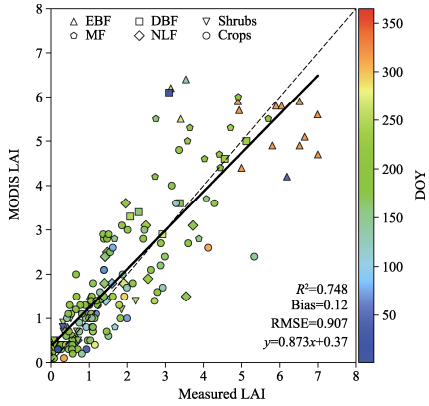

Figure 7 Scatter plot of MODIS product reprocessing dataset with ground truth LAI (Notes: EBF, evergreen broadleaf forest; DBF, deciduous broadleaf forest; Shrubs, Savanna; MF, mixed forest; NLF, needle-leaf forest; Crops: crops; DOY: julian day)

5 Discussion and Conclusion

MODIS LAI products have been extensively utilized in global change studies. However, inherent algorithmic limitations introduce uncertainty into these products, leading to errors in global change analyses. This study proposed a synthesis method based on the maximum FAPAR using the MODIS LAI product. By employing a spatiotemporal filtering technique, this study effectively reduced outliers and vacant values, resulting in a global LAI dataset characterized by spatiotemporal continuity and reliable quality. Validation using ground truth data showed that the optimized product had high accuracy, with a R^2 value of 0.748, bias of 0.119, and RMSE of 0.907, which were better than those of the existing product accuracy[3] (R^2=0.615, bias=0.13, and RMSE=1.16). Using the reprocessed dataset, this study uncovered the distribution pattern of global LAI in different seasons, elucidated the spatiotemporal variations of LAI in the Northern and Southern Hemispheres, and identified the growth regions of the global LAI over the past two decades. The primary growth regions include eastern China, India, and Europe.

The contribution of this study is the provision of a high-precision dataset that can facilitate further research on global climate change, the carbon cycle, the development of an ecological civilization, and the pursuit of dual carbon goals, particularly in China.

Author Contributions

Zhang, Y. H. and Gao, X. designed the algorithms of dataset. Liu, L., Zhang, Y. H. and Hu, Z. W. contributed to the data processing and analysis. Wang, J. Z. and Zhang, Y. H. preformed the data validation. Liu, L. and Zhang, Y. H. wrote the data paper.

Conflicts of Interest

The authors declare no conflicts of interest.

References

[1] Liu, Y., Liu, R., Chen, J., *et al*. Current status and perspectives of leaf area index retrieval from optical remote sensing data [J]. *Geo-information Science*, 2013, 15(5): 734–743.

[2] Chen, J. M., Black, T. A. Defining leaf area index for non-flat leaves [J]. *Plant, Cell & Environment*, 1992, 15(4): 421–429.

[3] Fang, H., Baret, F., Plummer, S., *et al*. An overview of global leaf area index (LAI): methods, products, validation, and applications [J]. *Reviews of Geophysics*, 2019, 57(3): 739–799.

[4] GCOS. The global observing system for climate implementation needs [R]. 2016.

[5] Xiao, Z., Liang, S., Wang, J., *et al*. Use of general regression neural networks for generating the glass leaf area index product from time-series MODIS surface reflectance [J]. *IEEE Transactions on Geoscience and Remote Sensing*, 2014, 52(1): 209–223.

[6] Baret, F., Hagolle, O., Geiger, B., *et al*. LAI, fAPAR and fCover CYCLOPES global products derived from VEGETATION [J]. *Remote Sensing of Environment*, 2007, 110(3): 275–286.

[7] Knyazikhin, Y., Martonchik, J. V., Myneni, R. B., *et al*. Synergistic algorithm for estimating vegetation canopy leaf area index and fraction of absorbed photosynthetically active radiation from MODIS and MISR data [J]. *Journal of Geophysical Research: Atmospheres*, 1998, 103(D24): 32257.

[8] Chen, C., Park, T., Wang, X., *et al*. China and India lead in greening of the world through land-use management [J]. *Nature Sustainability*, 2019, 2(2): 122–129.

[9] Zhang, Y., Hu, Z., Wang, J., *et al*. Temporal upscaling of MODIS instantaneous FAPAR improves forest gross primary productivity (GPP) simulation [J]. *International Journal of Applied Earth Observation and Geoinformation*, 2023, 121: 103360.

[10] Fang, H., Zhang, Y., Wei, S., *et al*. Validation of global moderate resolution leaf area index (LAI) products over croplands in northeastern China [J]. *Remote Sensing of Environment*, 2019, 233(4): 111377.

[11] Ma, P. P., Li, J., Liu, Q. H., *et al*. 2019. Multisensor synergistic quantitative leaf area index product of China. *Journal of Remote Sensing*, 23(6): 1232–1252.

[12] Yuan, H., Dai, Y., Xiao, Z., *et al*. Reprocessing the MODIS leaf area index products for land surface and climate modeling [J]. *Remote Sensing of Environment*, 2011, 115(5): 1171–1187.

[13] Wang, J., Yan, K., Gao, S., *et al*. Improving the quality of MODIS LAI products by exploiting spatiotemporal correlation information [J]. *IEEE Transactions on Geoscience and Remote Sensing*, 2023, 61: 1–19.

[14] Zhang, Y., Fang, H., Wang, Y., *et al*. Variation of intra-daily instantaneous FAPAR estimated from the geostationary Himawari-8 AHI data [J]. *Agricultural and Forest Meteorology*, 2021, 307: 108535.

[15] Pu, J., Yan, K., Gao, S., *et al*. Improving the MODIS LAI compositing using prior time-series information [J]. *Remote Sensing of Environment*, 2023, 287: 113493.

[16] Liu, L., Zhang, Y. H., Hu, Z. W., *et al*. MODIS global leaf area index product reprocessing dataset (2001–2021) [J/DB/OL]. *Digital Journal of Global Change Data Repository*, 2023. https://doi.org/10.3974/geodb.2023.10.03.V1. https://cstr.escience.org.cn/CSTR:20146.11.2023.10.03.V1.

[17] GCdataPR Editorial Office. GCdataPR data sharing policy[OL]. https://doi.org/10.3974/dp.policy.2014.05 (Updated 2017).

[18] Zeng, Y., Li, J., Liu, Q. Global LAI ground validation dataset and product validation framework [J]. *Advances in Earth Science*, 2012, 27(2): 165–174.

[19] Weiss, M., Baret, F., Block, T., *et al*. On line validation exercise (OLIVE): a web based service for the validation of medium resolution land products application to FAPAR products [J]. *Remote Sensing*, 2014, 6(5): 4190–4216.